ISSN 1007-9327 (print)
ISSN 2219-2840 (online)

World Journal of *Gastroenterology*

World J Gastroenterol 2019 May 7; 25(17): 2019-2148

Published by Baishideng Publishing Group Inc

World Journal of Gastroenterology

Contents

Weekly Volume 25 Number 17 May 7, 2019

CASE REPORT

Contents

World Journal of Gastroenterology

Volume 25 Number 17 May 7, 2019

ABOUT COVER

Editorial board member of *World Journal of Gastroenterology*, Gülsüm Özlem Elpek, MD, Professor, Department of Pathology, School of Medicine, Akdeniz University, Antalya 07070, Turkey

AIMS AND SCOPE

World Journal of Gastroenterology (*World J Gastroenterol*, *WJG*, print ISSN 1007-9327, online ISSN 2219-2840, DOI: 10.3748) is a peer-reviewed open access journal. The *WJG* Editorial Board consists of 642 experts in gastroenterology and hepatology from 59 countries.

The primary task of *WJG* is to rapidly publish high-quality original articles, reviews, and commentaries in the fields of gastroenterology, hepatology, gastrointestinal endoscopy, gastrointestinal surgery, hepatobiliary surgery, gastrointestinal oncology, gastrointestinal radiation oncology, *etc*. The *WJG* is dedicated to become an influential and prestigious journal in gastroenterology and hepatology, to promote the development of above disciplines, and to improve the diagnostic and therapeutic skill and expertise of clinicians.

INDEXING/ABSTRACTING

The *WJG* is now indexed in Current Contents®/Clinical Medicine, Science Citation Index Expanded (also known as SciSearch®), Journal Citation Reports®, Index Medicus, MEDLINE, PubMed, PubMed Central, Scopus and Directory of Open Access Journals. The 2018 edition of Journal Citation Report® cites the 2017 impact factor for *WJG* as 3.300 (5-year impact factor: 3.387), ranking *WJG* as 35th among 80 journals in gastroenterology and hepatology (quartile in category Q2).

RESPONSIBLE EDITORS FOR THIS ISSUE

Responsible Electronic Editor: *Yu-Jie Ma* **Proofing Editorial Office Director:** *Ze-Mao Gong*

NAME OF JOURNAL
World Journal of Gastroenterology

ISSN
ISSN 1007-9327 (print) ISSN 2219-2840 (online)

LAUNCH DATE
October 1, 1995

FREQUENCY
Weekly

EDITORS-IN-CHIEF
Subrata Ghosh, Andrzej S Tarnawski

EDITORIAL BOARD MEMBERS
http://www.wjgnet.com/1007-9327/editorialboard.htm

EDITORIAL OFFICE
Ze-Mao Gong, Director

PUBLICATION DATE
May 7, 2019

INSTRUCTIONS TO AUTHORS
https://www.wjgnet.com/bpg/gerinfo/204

GUIDELINES FOR ETHICS DOCUMENTS
https://www.wjgnet.com/bpg/GerInfo/287

GUIDELINES FOR NON-NATIVE SPEAKERS OF ENGLISH
https://www.wjgnet.com/bpg/gerinfo/240

PUBLICATION MISCONDUCT
https://www.wjgnet.com/bpg/gerinfo/208

ARTICLE PROCESSING CHARGE
https://www.wjgnet.com/bpg/gerinfo/242

STEPS FOR SUBMITTING MANUSCRIPTS
https://www.wjgnet.com/bpg/GerInfo/239

ONLINE SUBMISSION
https://www.f6publishing.com

World Journal of Gastroenterology

Submit a Manuscript: https://www.f6publishing.com

World J Gastroenterol 2019 May 7; 25(17): 2071-2085

DOI: 10.3748/wjg.v25.i17.2071

ISSN 1007-9327 (print) ISSN 2219-2840 (online)

ORIGINAL ARTICLE

Basic Study

Herbs-partitioned moxibustion alleviates aberrant intestinal epithelial cell apoptosis by upregulating A20 expression in a mouse model of Crohn's disease

Jing Zhou, Lu-Yi Wu, Liu Chen, Ya-Jing Guo, Yi Sun, Tao Li, Ji-Meng Zhao, Chun-Hui Bao, Huan-Gan Wu, Yin Shi

ORCID number: Jing Zhou (0000-0003-0495-2175); Lu-Yi Wu (0000-0002-7297-2509); Liu Chen (0000-0003-3853-6612); Ya-Jing Guo (0000-0003-0627-9236); Yi Sun (0000-0001-7705-219X); Tao Li (0000-0001-6313-3829); Ji-Meng Zhao (0000-0001-9075-6036); Chun-Hui Bao (0000-0002-9763-0046); Huan-Gan Wu (0000-0003-1725-6881); Yin Shi (0000-0002-7502-1573).

Author contributions: Zhou J, Shi Y, and Wu HG designed the research; Zhou J, Chen L, Zhao JM, Guo YJ, Sun Y, and Li T performed the experiments; Wu LY, Zhou J, and Bao CH collected and analyzed the data; Zhou J wrote the manuscript; all authors reviewed the manuscript prior to its submission, and read and approved the final manuscript.

Supported by National Natural Science Foundation of China, No. 81273844 and No. 81473757; National Key Basic Research Program of China (973 Program), No. 2015CB554500; and Shanghai Rising-Star Program, No. 16QA1403400.

Institutional animal care and use committee statement: All animal experiments in this study were performed under guidelines approved by the Animal Ethics Committee of the Shanghai University of Traditional Chinese Medicine (No. 2013025).

Conflict-of-interest statement: The

Jing Zhou, Liu Chen, Ya-Jing Guo, Yi Sun, Tao Li, Graduate School, Shanghai University of Traditional Chinese Medicine, Shanghai 201203, China

Lu-Yi Wu, Qigong Institute, Shanghai University of Traditional Chinese Medicine, Shanghai 200030, China

Ji-Meng Zhao, Chun-Hui Bao, Huan-Gan Wu, Yin Shi, Key Laboratory of Acupuncture and Immunological Effects, Shanghai University of Traditional Chinese Medicine, Shanghai 201203, China

Ji-Meng Zhao, Chun-Hui Bao, Huan-Gan Wu, Key Laboratory of Acupuncture and Immunological Effects, Shanghai Institute of Acupuncture-Moxibustion and Meridian, Shanghai 200030, China

Yin Shi, Outpatient Department, Shanghai Institute of Acupuncture-Moxibustion and Meridian, Shanghai 200030, China

Corresponding author: Yin Shi, PhD, Doctor, Professor, Outpatient Department, Shanghai Institute of Acupuncture-Moxibustion and Meridian, 650 South Wanping Road, Shanghai 200030, China. flysy0636@163.com
Telephone: +86-21-64383910
Fax: +86-21-64390339

Abstract

BACKGROUND

A20 inhibits intestinal epithelial cell apoptosis in Crohn's disease, and herbs-partitioned moxibustion (HPM) has been demonstrated to be an effective treatment for Crohn's disease. However, the mechanism by which HPM reduces intestinal epithelial cell apoptosis in Crohn's disease has not been thoroughly elucidated to date.

AIM

To elucidate whether HPM exerts its effects by upregulating A20 to affect intestinal epithelial cell apoptosis in a Crohn's disease mouse model.

METHODS

In this study, mice with A20 deletion in intestinal epithelial cells ($A20^{IEC\text{-}KO}$) were utilized to establish a Crohn's disease mouse model with 2,4,6-trinitrobenzene

authors declare no conflicts of interest.

Data sharing statement: No additional data are available.

ARRIVE guidelines statement: The manuscript was prepared according to the ARRIVE guidelines.

Manuscript source: Unsolicited manuscript

Received: January 13, 2019
Peer-review started: January 14, 2019
First decision: February 13, 2019
Revised: March 13, 2019
Accepted: March 15, 2019
Article in press: March 16, 2019
Published online: May 7, 2019

P-Reviewer: Abdolghaffari AH
S-Editor: Ma RY
L-Editor: Wang TQ
E-Editor: Ma YJ

sulfonic acid (TNBS) administration, as well as wild-type mice. Mice were randomly divided into normal control (NC), model control (MC), mesalazine (MESA), and HPM groups. The morphology of the colonic mucosa was observed by hematoxylin-eosin staining, and serum endotoxin and apoptosis of epithelial cells were evaluated by enzyme-linked immunosorbent assay and terminal dUTP nick-end labeling assay accordingly. The protein expression levels of A20 and tumor necrosis factor receptor 1 (TNFR1)-related signaling molecules were evaluated by Western blot, and co-expression of A20 and TNFR1-associated death domain (TRADD) and co-expression of A20 and receptor-interacting protein 1 (RIP1) were observed by double immunofluorescence staining.

RESULTS

The intestinal epithelial barrier was noted to have an improvement in the HPM group of wild-type (WT) mice compared with that in $A20^{IEC\text{-}KO}$ mice. Compared with $A20^{IEC\text{-}KO}$ HPM mice, serum endotoxin levels and apoptosis percentages were decreased ($P < 0.01$), A20 expression levels were increased ($P < 0.01$), and expression of TNFR1, TRADDD, and RIP1 was decreased in the HPM group of WT mice ($P_{TNFR1} < 0.05$, $P_{TRADD} < 0.01$, $P_{RIP1} < 0.01$). Both of the co-expression of A20/TRADD and A20/RIP1 showed a predominantly yellow fluorescence in the HPM group of WT mice, while a predominantly red fluorescence was noted in the HPM group of $A20^{IEC\text{-}KO}$ mice.

CONCLUSION

Our findings suggest that HPM in treating Crohn's disease functions possibly via upregulation of the A20 expression level, resulting in downregulation of TNFR1, TRADD, and RIP1 to alleviate increased cell apoptosis in the intestinal epithelial barrier in Crohn's disease.

Key words: Herbs-partitioned moxibustion; Crohn's disease; Apoptotic pathway; Inflammation; A20

Core tip: We report our results derived from mice with A20 deletion in intestinal epithelial cells by inducing Crohn's disease. The Crohn's disease model was induced with 2,4,6-trinitrobenzene sulfonic acid. This study demonstrates for the first time that herbs-partitioned moxibustion can upregulate the expression of A20, resulting in downregulation of tumor necrosis factor receptor (TNFR) 1, TNFR1-associated death domain, and receptor-interacting protein 1 to alleviate increased cell apoptosis in the intestinal epithelial barrier in Crohn's disease.

Citation: Zhou J, Wu LY, Chen L, Guo YJ, Sun Y, Li T, Zhao JM, Bao CH, Wu HG, Shi Y. Herbs-partitioned moxibustion alleviates aberrant intestinal epithelial cell apoptosis by upregulating A20 expression in a mouse model of Crohn's disease. *World J Gastroenterol* 2019; 25(17): 2071-2085
URL: https://www.wjgnet.com/1007-9327/full/v25/i17/2071.htm
DOI: https://dx.doi.org/10.3748/wjg.v25.i17.2071

INTRODUCTION

Crohn's disease is a chronic inflammatory bowel disease with symptoms of abdominal pain, diarrhea, weight loss, perianal lesions, and anemia[1]. In the past ten years, Crohn's disease has increased significantly as a worldwide health problem[2]. The highest reported prevalence areas are Europe and North America with 322 cases per 100000[3,4]. The high prevalence and long-term nature of the disease pose a great burden on patients and the society, due to health-related reduction in quality of life and decreased economic productivity, which calls for high-quality and cost-efficient care for patients.

Crohn's disease most likely results from complex interactions between genetics, environment, and gut microbiota, which lead to dysfunction of the epithelial barrier

with consequent deregulation of the mucosal immune system and responses to gut microbiota[5,6]. The intestinal epithelium is a notably large mucosal surface with a strong capacity for self-renewal[7,8]. Proliferation of progenitor cells and their differentiation into mature epithelial cells continuously recompense cell losses[9]. However, in Crohn's disease, this homeostasis is disrupted by increased apoptosis of epithelial cells due to increased stimulation of the immune system, leading to loss of epithelial integrity and local inflammation[10]. In many patients with Crohn's disease, epithelial injury and inflammation due to increased cell apoptosis depend on tumor necrosis factor (TNF)[11]. TNF-alpha (TNF-α), a transmembrane protein, binds to its ligand, TNF receptor (TNFR) 1, recruiting TNFR1-associated death domain (TRADD) and receptor-interacting protein (RIP). In turn, TRADD and RIP associate with FAS-associated death domain protein (FADD) to activate caspase 8, leading to apoptosis[12]. Studies have shown that lower expression of A20 correlates with improved anti-TNF-α drug responses[13], and mice with A20 deletion in intestinal epithelial cells ($A20^{IEC\text{-}KO}$) are hypersensitive to TNF-α-induced intestinal epithelial apoptosis[14]. These studies have revealed a negative regulatory role of A20 in the TNF-α-induced apoptosis pathway.

A20 is a cytoplasmic protein that was originally identified as a primary TNF-α-induced responsive molecule in endothelial cells and negatively regulates NF-κB-dependent gene expression in response to stimuli, such as TNF-α and interleukin-1 (IL-1)[15,16]. A20 contains an N-terminal ovarian tumor deubiquitinating and E3 ubiquitin ligase activity toward the death-domain-containing protein kinase RIP1 and adaptor proteins in the TNF-α/TNFR1 pathway, and is the most important anti-apoptotic protein involved in diseases such as Crohn's disease[17,18] and glioblastoma[19]. A20 inhibits TNF-α-induced apoptosis by disrupting recruitment of TRADD and RIP1 to the TNFR1 complex[19]. It has been reported that $A20^{IEC\text{-}KO}$ mice are normal, but they are more likely to suffer from intestinal injury induced by intraperitoneal TNF-α injection[13,14]. Furthermore, clinical studies show that the mucosal expression of A20 was significantly lower in Crohn's disease patients compared to healthy controls[13,17]. Taken together, these findings indicate that A20 expression levels are critical in maintaining epithelial barrier function, which may provide a molecular mechanism for illustrating apoptosis in the development of Crohn's disease.

Despite the effectiveness of Western medications, such as aminosalicylates and thiopurines, in inducing and maintaining remission in Crohn's disease, they are limited by their serious side effects, such as nausea, bone marrow suppression, hepatitis, allergic reaction, pancreatitis, and infections and opportunistic infections[20-24]. Approximately 10%-26% of patients withdraw from these treatments because of the adverse effects[23,25]. Thus, a safer therapy is necessary for managing the disease. Moxibustion, a traditional Chinese medicine, has been demonstrated to be an effective and safe method in treating mild and moderate active-phase Crohn's disease with long-term clinical efficacy[26-28]. After 12 wk of herbs-partitioned moxibustion (HPM) therapy, 74% of 46 mild and moderate Crohn's disease patients [Crohn's disease Activity Index (CDAI) from 151 to 350] entered remission periods (CDAI scores < 150). In addition, moxibustion can effectively relieve symptoms such as abdominal pain and diarrhea and can increase hemoglobin counts and decrease C-reactive protein levels[28]. No adverse events were reported in these studies. We previously demonstrated that HPM improved intestinal epithelial barrier function by downregulating the apoptosis of intestinal epithelial cells[29].

However, whether HPM regulates A20 expression to downregulate intestinal epithelial cell apoptosis in Crohn's disease is obscure. Thus, we used HPM and the most frequently prescribed medication, mesalazine (an aminosalicylate)[24], in both $A20^{IEC\text{-}KO}$ and wild-type (WT) Crohn's disease mice to evaluate the efficacy of HPM in upregulating A20 expression in an apoptotic pathway induced by TNF-α/TNFR1.

MATERIALS AND METHODS

Animals

Eight-week-old $A20^{IEC\text{-}KO}$ and WT C57BL/6 mice were obtained from the Shanghai Model Organisms Center (Shanghai, China). The mice were housed at the animal care center of the Shanghai University of Traditional Chinese Medicine and were provided with humane care in a temperature-controlled room (temperature of 22 ± 1 °C and humidity 50% ± 70%) under a 12-h light–dark cycle with free access to food and water. All animal experiments in this study were performed under guidelines approved by the Animal Ethics Committee of the Shanghai University of Traditional Chinese Medicine (No. 2013025).

Establishment of a mouse model of Crohn's disease

Forty-eight C57BL/6 WT and A20^{IEC-KO} mice each were randomly divided into normal control (NC, n = 12), model control (MC, n = 12), mesalazine (MESA, n = 12), and HPM (n = 12) groups. The MC, MESA, and HPM groups were administered with 2,4,6-trinitrobenzene sulfonic acid (TNBS) enemas to establish an experimental Crohn's disease model[30]. The enema solution was prepared with absolute ethanol and 5% TNBS at a 1:1 proportion. The solution was stored away from light. Mice were provided access to water only for 24 h prior to TNBS administration and were weighed. Mice were then anesthetized with 0.05 mL/10 g of 1% pentobarbital sodium via intraperitoneal injection. All mice apart from NC group mice were administered TNBS/ethanol (0.06 mL/10 g of TNBS + 50% ethanol 0.25 mL) intra-anally via a rubber tube, and the solution was retained in the gut cavity at a depth of 3-4 cm. NC mice were administered with physiological saline at 0.05 mL/10 g. All mice were fixed in a handstand posture for 2 min after the rubber tube was withdrawn to prevent outflow of solution. This procedure was performed once. Two mice were randomly selected from each group and sacrificed to confirm the presence of Crohn's disease-like intestinal pathology by hematoxylin and eosin stain (H&E) staining after 4 d.

Treatment methods

Upon confirmation of the model establishment, HPM group mice were treated with HPM. Moxa cones (0.5 cm in diameter and 0.3 cm high) made of refined mugwort floss were placed on herbal cakes [*e.g.*, medicinal formula dispensing (radix) Aconiti praeparata, (cortex) Cinnamomi] at Tianshu (ST25) and Qihai (CV6) acupuncture points (which regulate intestinal functions) and ignited. Two moxa cones were used per treatment, which was administered once daily for 10 d. MESA group mice were fed MESA, which was prepared at a proportion of 1:0.0026[31], twice daily for 10 d. Mice in the MC and NC groups did not undergo any treatment.

Histological observation

All mice were sacrificed simultaneously at the conclusion of treatment. Approximately 4 cm of colon lesions were resected at a 3-4 cm distance from the anus. A 1 cm length of the dissected colon was removed, washed with iced saline, fixed in 10% natural buffered formalin solution, embedded in paraffin, cut into tissue sections, and stained with H&E. Obtained images were observed under a light microscope (Olympus, Tokyo, Japan).

Enzyme-linked immunosorbent assay

A 96-well commercial kit (MyBioSource, Inc. San Diego, CA, United States) was applied to evaluate serum endotoxin levels. Blood samples were centrifuged at 3000 × g for 10 min. Diluted serum sample (1:10), endotoxin test water, and TAL were added to the plate and incubated for 10 min at 37 °C. Then, chromogenic matrix solution was added to the plate and incubated for 6 min at 37 °C. After that, azo reagent was added to the plate and incubated for 5 min at 37 °C. Optical densities were detected with a plate reader (BioTek Instruments, Winooski, VT, United States)

Western blot analysis

Protein (60 μg) extracted from isolated rat intestinal epithelial cell samples was separated by SDS-PAGE and transferred to polyvinylidene difluoride (PVDF) membranes. The membranes were then blocked with 5% skimmed milk in TBS-T for 1 h at room temperature and incubated with the following primary antibodies overnight at 4 °C: A20 (1:1000; ab13597, Abcam), TNF-α (1:1000; ab6671, Abcam), TNFR1 (1:5000; ab19139, Abcam), TRADD (1:500; ab110644, Abcam), RIP1 (1:500; ab72139, Abcam), FADD (1:400; ab24533, Abcam), and GAPDH (1:1500; 5174, CST). Following several sequential washes, the membranes were incubated with the corresponding secondary anti-mouse antibody (A0208, Beyotime) for 1 h at room temperature. Blots were then washed four times with TBS-T (10 min each time). The membranes were stained with ECL enhanced chemiluminescence solution and visualized using a visualizer.

Terminal dUTP nick-end labeling assay

A terminal dUTP nick-end labeling (TUNEL) kit purchased from MyBioSource was utilized to evaluate apoptosis. Paraffin sections were first fully deparaffinized and hydrated, treated with protease K solution (20 μg/mL) for 15 min at room temperature, and subsequently washed and immersed in 3% hydrogen peroxide for 15 min. The sections were then immersed in an equilibrium buffer for 20 min at room temperature and afterward incubated with TdTase for 60 min at 37 °C. After that, the sections were stained with 3,3'-diaminobenzidine (DAB, Shanghai Long Island Biotec.

Co., Ltd, China) and counterstained with hematoxylin. Apoptotic cells as well as the total number of cells were calculated.

Double immunofluorescence staining

Paraffin sections were fully deparaffinized and hydrated, and then washed and heated to 92-98 °C for antigen retrieval. Samples were incubated with primary antibodies against A20 (ab13597, Abcam), RIP1 (ab72139, Abcam), and TRADD (ab110644, Abcam) in blocking buffer overnight at 4 °C. Samples were subsequently incubated with the corresponding secondary antibody in blocking buffer at room temperature, and finally incubated with DAPI staining solution for 10 min. Images were obtained under a fluorescence microscope (Nikon, Japan).

Statistical analysis

Experimental data were analyzed with SPSS 21.0 software (SPSS Inc., Wacker Drive, Chicago, IL, Uinted States) and GraphPad Prism 5 (GraphPad Software, San Diego, CA, Uinted States). All data are presented as the mean ± standard deviation (SD). Statistics among each experimental group were analyzed using one-way analysis of variance (ANOVA) followed by the least significant difference test. The level of significance was set at $a = 0.05$ and $^{a}P < 0.05$, $^{b}P < 0.01$; $^{c}P < 0.05$, $^{d}P < 0.01$; $^{e}P < 0.05$, $^{f}P < 0.01$; $^{g}P < 0.05$, $^{h}P < 0.01$.

RESULTS

Intestinal morphological observations in each group

Previous studies have shown that the Crohn's disease model of A20$^{IEC\text{-}KO}$ mice showed a more severely damaged mucosa than WT mice[13]. In this study, by histopathological evaluation, we found that in WT NC mice, intact mucosal epithelial cells and normal morphological changes affecting the submucosa and muscularis were observed (Figure 1A). In WT MC mice, sparse goblet cells, fibrous hyperplasia, as well as damage to mucosal glands, vasodilation, and hyperemia were noted in the mucosa, and hyperemia and edema were observed under the submucosa (Figure 1B). In WT MESA mice, sparse goblet cells, infiltration of inflammatory cells into the mucosa and submucosa, as well as hyperemia and edema under the submucosa were noted. No obvious abnormal changes were observed in the structural morphology of mucosal, submucosal, and muscularis layers (Figure 1C). In WT HPM mice, sparse goblet cells, mild infiltration of inflammatory cells into the colonic mucosa and submucosa, sparse fibroblast hyperplasia, and healing ulcers were observed. No obvious abnormal changes were observed in the structural morphology of the mucosal, submucosal, or muscularis layer (Figure 1D).

In A20$^{IEC\text{-}KO}$ NC mice, intact mucosal epithelial cells and normal submucosal and muscularis structural morphology were observed (Figure 1E). In A20$^{IEC\text{-}KO}$ MC mice, partial epithelial cells loss, mucosal goblet cell depletion, inflammatory cell infiltration, glandular damage, and proliferation of fibrous tissue were observed in the mucosa in addition to erosion and necrosis of the mucosal surface. Hyperemia and edema were observed in both mucosal and submucosal layers (Figure 1F). In A20$^{IEC\text{-}KO}$ MESA mice, sparse goblet cells, small healing ulcers with associated glandular destruction, and massive inflammatory cell infiltration were observed in the mucosa. No obviously abnormal structural changes in the mucosal, submucosal, or muscularis layer were observed (Figure 1G). In A20$^{IEC\text{-}KO}$ HPM mice, sparse goblet cells, inflammatory cell infiltration, and proliferation of fibrous tissue were observed in mucosal tissue. No obviously abnormal structural changes in the mucosal, submucosal, or muscularis layer were noted (Figure 1H).

Variations in epithelial permeability across groups

Next, we observed the intestinal epithelial barrier permeability by detecting serum endotoxin levels(Figure 2). In WT groups, as compared with NC mice, serum endotoxin levels were upregulated in the MC, MESA, and HPM groups ($P_{MC} < 0.01$, $P_{MESA} < 0.01$, $P_{HPM} < 0.01$). Serum endotoxin levels were downregulated in HPM ($P < 0.01$) and MESA ($P < 0.05$) mice as compared to MC mice. Serum endotoxin levels were significantly decreased in HPM mice ($P < 0.01$) as compared to MESA mice.

In mice from A20$^{IEC\text{-}KO}$ groups, as compared with NC mice, serum endotoxin levels were upregulated in the MC, MESA, and HPM groups ($P_{MC} < 0.01$, $P_{MESA} < 0.01$, $P_{HPM} < 0.01$). They were downregulated in MESA and HPM mice as compared to MC mice ($P_{MESA} < 0.01$, $P_{HPM} < 0.01$). Serum endotoxin levels were significantly decreased in HPM mice ($P < 0.01$) as compared to those of the MESA group.

Compared with WT NC mice, no significant difference in serum endotoxin levels were noted in NC A20$^{IEC\text{-}KO}$ mice ($P > 0.05$). Compared with WT MC mice, endotoxin

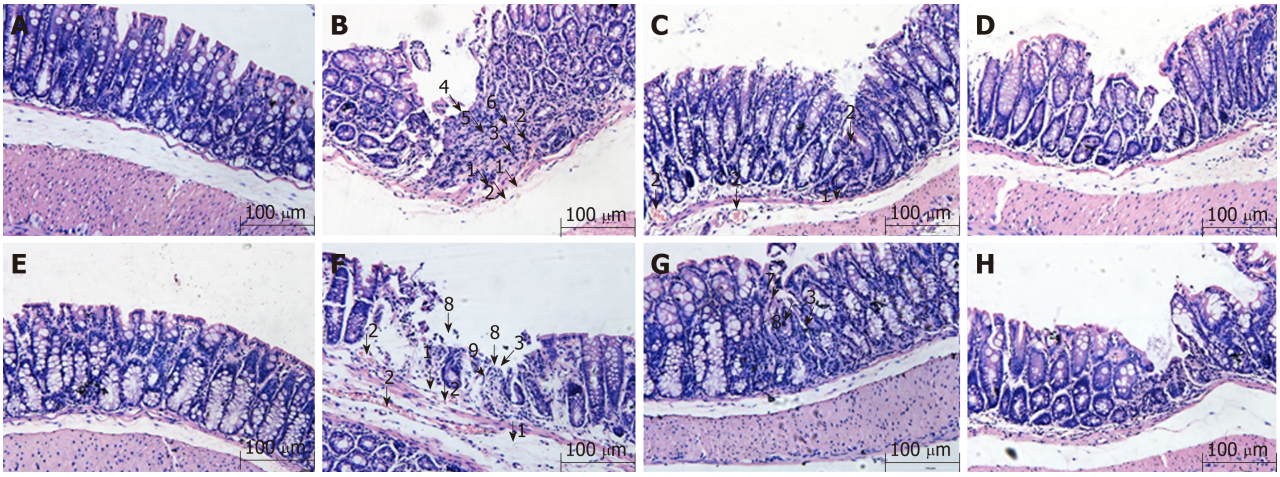

Figure 1 Histological observation of intestinal epithelial tissues across groups (magnification,×100). A: Wild-type mice in normal control group; B: Wild-type mice in model control group; C: Wild-type mice in mesalazine group; D: Wild-type mice in herbs-partitioned moxibustion group; E: A20^{IEC-KO} mice in normal control group; F: A20^{IEC-KO} mice in model control group; G: A20^{IEC-KO} mice in mesalazine group; H: A20^{IEC-KO} mice in herbs-partitioned moxibustion group. 1: Tissue edema; 2: Hyperemia; 3: Inflammatory cell infiltration; 4: Necrosis; 5: Granulation tissue proliferation; 6: Destruction of glandular structure; 7: Healing ulcer; 8: Ulcer; 9: Proliferation of fibrous tissue.

levels in MC A20^{IEC-KO} mice were upregulated ($P < 0.05$). Compared with WT HPM mice, serum endotoxin levels were upregulated in HPM A20^{IEC-KO} mice ($P < 0.01$).

Observation of percentage of apoptotic intestinal epithelial cells in each group

Since A20 protein is involved in epithelial barrier function by its anti-apoptotic role in Crohn's disease, we observed cell apoptosis percentage in different groups by TUNEL method. In WT groups, as compared with NC mice, apoptosis percentages were significantly increased in the MC, MESA, and HPM groups ($P_{MC} < 0.01$, $P_{MESA} < 0.01$, $P_{HMP} < 0.01$). Apoptosis percentages were significantly decreased in MESA and HPM mice ($PMESA < 0.01$, $PHPM < 0.01$) as compared to those of the MC group. No significant difference in apoptosis percentages was noted in HPM mice ($P > 0.05$) (Figure 3A-D, I) as compared to those of the MESA group.

In A20^{IEC-KO} groups, as compared with NC mice, apoptosis percentages were significantly increased in the MC, MESA, and HPM groups ($P_{MC} < 0.01$, $P_{MESA} < 0.01$, $P_{HPM} < 0.01$). Apoptosis percentages were significantly decreased in the MESA and HPM groups ($P_{MESA} < 0.01$, $P_{HPM} < 0.01$) as compared to the MC group. There was no difference between the HPM and MESA groups ($P > 0.05$) (Figure 3E-I).

Compared with each corresponding group of WT mice, apoptosis percentages were significantly increased in the NC, MC, MESA, and HPM groups of A20^{IEC-KO} mice ($P_{NC} < 0.01$, $P_{MC} < 0.01$, $P_{MESA} < 0.01$, $P_{HPM} < 0.01$) (Figure 3A-I).

Expression of members of the TNF-α/TNFR1-TRADD-FADD apoptotic pathway in the intestinal epithelium across groups

A20 expression across groups: In WT groups, as compared with the NC group, A20 levels were decreased in MC, MESA ($P_{MC} < 0.01$, $P_{MESA} < 0.01$), and HPM mice ($P_{HPM} < 0.05$). Compared with MC mice, A20 expression was significantly increased in HPM mice ($P < 0.01$) and increased in MESA mice ($P < 0.05$). Compared with MESA mice, no difference in A20 levels was noted in HPM mice ($P > 0.05$) (Figure 4A). No significant differences in A20 expression was noted among A20^{IEC-KO} groups ($PNC > 0.05$, $PMC > 0.05$, $PMESA > 0.05$, $PHPM > 0.05$) (Figure 4A). Compared with each corresponding group of WT mice, A20 expression levels were significantly decreased in all A20^{IEC-KO} groups ($P_{NC} < 0.01$, $P_{MC} < 0.01$, $P_{MESA} < 0.01$, $P_{HPM} < 0.01$) (Figure 4A).

TNF-α expression across groups: In WT groups, as compared with NC mice, TNF-α levels were significantly increased in MC, MESA, and HPM mice ($P_{MC} < 0.01$, $P_{MESA} < 0.01$, $P_{HPM} < 0.01$). Compared with MC mice, they were significantly decreased in MESA and HPM mice ($P_{MC} < 0.01$, $P_{MESA} < 0.01$). No differences in TNF-α expression in HPM mice were found as compared to those of the MESA group ($P > 0.05$) (Figure 4B).

In A20^{IEC-KO} groups, TNF-α levels were significantly increased in the MC, MESA, and HPM groups as compared to those in NC mice ($P_{MC} < 0.01$, $P_{MESA} < 0.01$, $P_{HMP} < 0.01$). TNF-α levels were significantly decreased in MESA and HPM mice ($P_{MESA} < 0.01$, $P_{HMP} < 0.01$) as compared to MC mice. TNF-α levels were decreased in HPM mice as

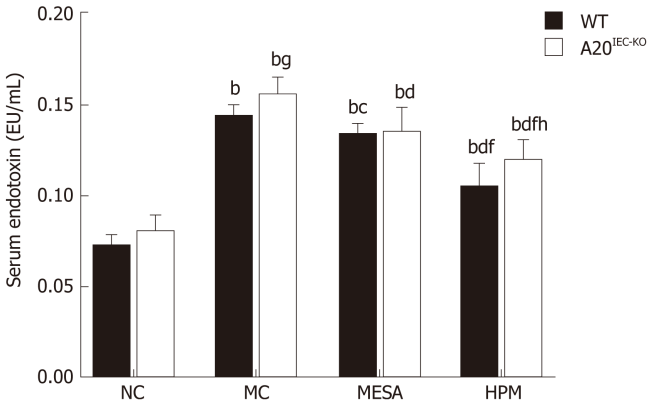

Figure 2 Serum endotoxin levels in mice across groups. Data are presented as the mean ± standard deviation (n = 10). Data were evaluated for statistical significance by one-way analysis of variance and are represented as follows: ^{a}P<0.05, ^{b}P < 0.01 as compared to normal control; ^{c}P < 0.05, ^{d}P < 0.01 as compared to model control; ^{e}P < 0.05, ^{f}P < 0.01 as compared to mesalazine; ^{g}P < 0.05, ^{h}P < 0.01 as compared to wild type. WT: Wild type; NC: Normal control; MC: Model control; MESA: Mesalazine; HPM: Herbs-partitioned moxibustion.

compared to those of the MESA group (P < 0.05) (Figure 4B). Compared with each corresponding group of WT mice, TNF-α levels in the A20^{IEC-KO} NC and HPM groups were not different (P > 0.05); TNF-α expression was increased in MC mice (P < 0.05) and significantly increased in MESA mice (P < 0.01) (Figure 4B).

TNFR1 expression across groups: In WT groups, as compared with NC mice, TNFR1 expression was significantly increased in MC, MESA, and HPM mice (P_{MC} < 0.01, P_{MESA} < 0.01, P_{HPM} < 0.05). Compared with MC mice, TNFR1 expression was significantly decreased in mice of the MESA and HPM groups (P_{MESA} < 0.01, P_{HMP} < 0.01). No difference in TNFR1 expression was found in HPM mice as compared to those of the MESA group (P > 0.05) (Figure 4C). In the A20^{IEC-KO} groups, as compared with NC mice, TNFR1 expression was significantly increased in MC and HPM mice (P_{MC} < 0.01, P_{HPM} < 0.01). It was increased in MESA mice as well (P_{MESA} < 0.05). Compared with MC mice, TNFR1 expression was significantly decreased in mice of the MESA and HPM groups (P_{MESA} < 0.01, P_{HMP} < 0.01). No difference in TNFR1 expression in mice of the HPM group was noted as compared to that in the MESA group (P > 0.05) (Figure 4C). Compared with the corresponding WT MC and WT HPM groups, TNFR1 expression was increased in A20^{IEC-KO} mice (PMC < 0.05, $PHPM$ < 0.05). No difference in TNFR1 expression among corresponding WT and A20^{IEC-KO} NC and MESA groups was noted (PNC > 0.05, $PMESA$ > 0.05) (Figure 4C).

TRADD expression across groups: In WT groups, as compared with NC mice, TRADD expression was significantly increased in MC and MESA mice (P_{MC} < 0.01, P_{MESA} < 0.01) and increased in HPM mice (P_{HMP} < 0.05). TRADD levels were significantly decreased in mice of the HPM group (P < 0.01) and decreased in those of the MESA group (P < 0.05) as compared to those of the MC group. Compared with MESA group mice, no difference in TRADD expression in HPM group mice was noted (P > 0.05) (Figure 4D). In A20^{IEC-KO} groups, compared with NC mice, TRADD levels were significantly increased in MC, MESA, and HPM mice (P_{MC} < 0.01, P_{MESA} < 0.01, P_{HPM} < 0.01). No difference in TRADD levels among the MC, MESA, and HPM groups was noted (P > 0.05) (Figure 4D). Compared with WT NC mice, no difference in TRADD expression was found in the same group of A20^{IEC-KO} mice (P > 0.05). TRADD expression was found to be significantly increased in MESA and HPM group mice (P_{MESA} < 0.01, P_{HPM} < 0.01) and increased in MC group A20^{IEC-KO} mice (P < 0.05) when compared to corresponding WT groups (Figure 4D).

RIP1 expression across groups: In WT groups, compared with NC group mice, RIP1 levels were significantly increased in the MC, MESA, and HPM groups (P_{MC} < 0.01, P_{MESA} < 0.01, P_{HPM} < 0.01). Compared with MC group mice, RIP1 levels were decreased in those of the HPM group (P < 0.05); no difference in RIP1 levels (P > 0.05) was noted in MESA group mice. Compared with MESA group mice, no difference in RIP1 levels was noted in those of the HPM group (P > 0.05) (Figure 4E). In mice of A20^{IEC-KO} groups, compared with those of the NC group, RIP1 levels were significantly increased in MC, MESA, and HPM mice (P_{MC} < 0.01, P_{MESA} < 0.01, P_{HPM} < 0.01). No differences in RIP1 levels among the MC, MESA, and HPM groups were noted (P > 0.05) (Figure 4E). Compared with WT NC mice, no difference in RIP1 expression in

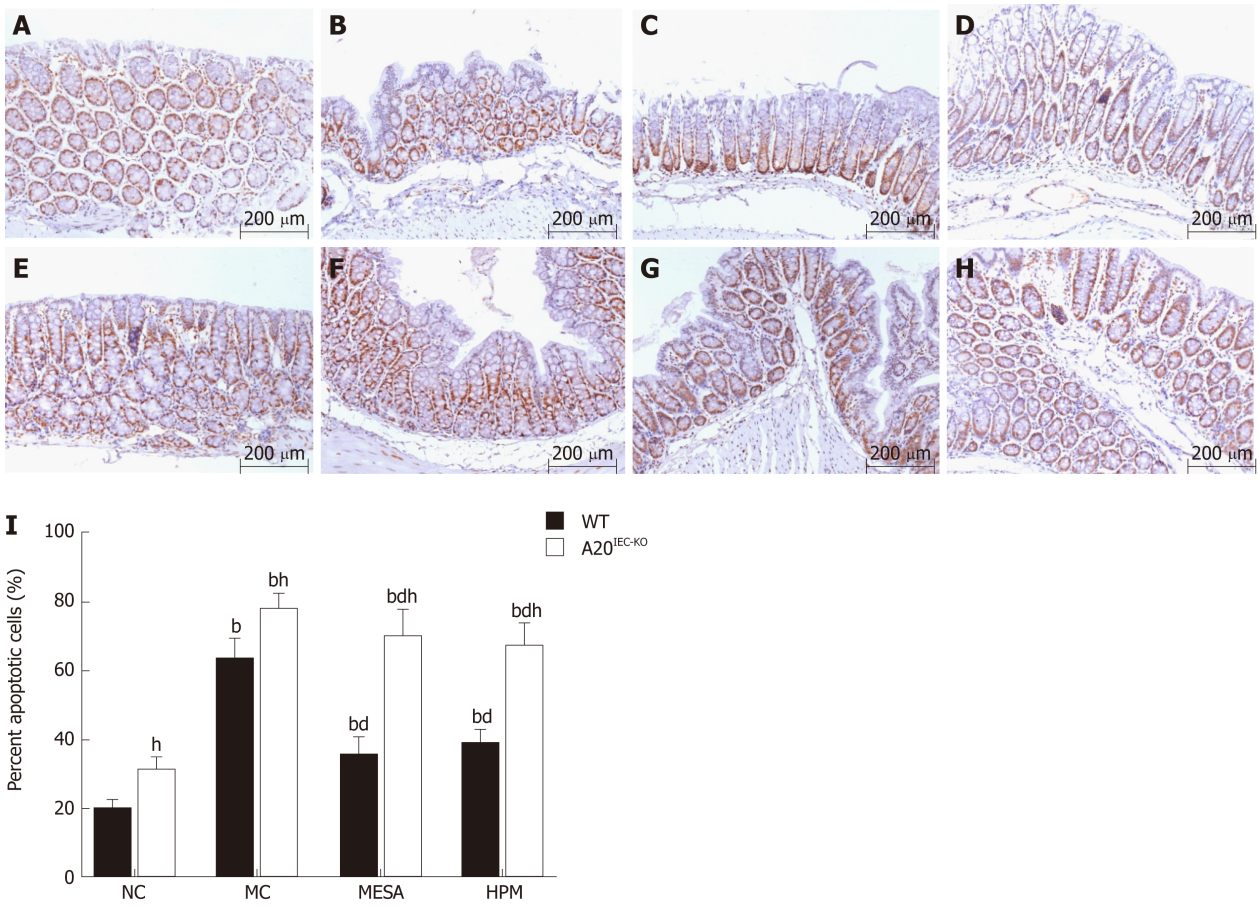

Figure 3 Apoptosis percentages of intestinal epithelial cells across groups (magnification,×200). A: Wild-type mice in normal control group; B: Wild-type mice in model control group; C: Wild-type mice in mesalazine group; D: Wild-type mice in herbs-partitioned moxibustion; E: A20^{IEC-KO} mice in normal control group; F: A20^{IEC-KO} mice in model control group; G: A20^{IEC-KO} mice in mesalazine group; H: A20^{IEC-KO} mice in herbs-partitioned moxibustion group; I: Percentage of apoptotic cells. Data are presented as the mean ± standard deviation (n = 10). Data were evaluated for statistical significance by one-way analysis of variance and are represented as follows: $^{a}P < 0.05$, $^{b}P < 0.01$ as compared to normal control; $^{c}P < 0.05$, $^{d}P < 0.01$ as compared to model control; $^{e}P < 0.05$, $^{f}P < 0.01$ as compared to mesalazine; $^{g}P < 0.05$, $^{h}P < 0.01$ as compared to wild type. WT: Wild type; NC: Normal control; MC: Model control; MESA: Mesalazine; HPM: Herbs-partitioned moxibustion.

A20^{IEC-KO} NC mice ($P > 0.05$) was found. Compared with WT HPM mice, expression of RIP1 was increased in A20^{IEC-KO} HPM mice ($P < 0.01$). Compared with corresponding WT MC and MESA mice, RIP1 expression was increased in A20^{IEC-KO} mice ($P_{MC} < 0.05$, $P_{MESA} < 0.05$) (Figure 4E).

FADD expression across groups: In WT groups, compared with NC mice, FADD levels were significantly increased in MC, MESA, and HPM mice ($P_{MC} < 0.01$, $P_{MESA} < 0.01$, $P_{HPM} < 0.01$). Compared with MC mice, FADD expression was decreased in MESA and HPM mice ($P_{MESA} < 0.01$, $P_{HPM} < 0.01$). Compared with mice of the MESA group, no difference in FADD expression levels was found in HPM mice ($P > 0.05$) (Figure 4F). In the A20^{IEC-KO} groups, compared with NC mice, FADD levels were significantly increased in MC, MESA, and HPM mice ($P_{MC} < 0.01$, $P_{MESA} < 0.01$, $P_{HPM} < 0.01$). No difference in FADD expression was noted among MC, MESA, and HPM mice ($P > 0.05$) (Figure 4F). Compared with WT NC and MC mice, no difference in FADD levels was found between A20^{IEC-KO} NC and MC mice ($PNC > 0.05$, $PMC > 0.05$). Compared with WT HPM mice, FADD levels were significantly increased in A20^{IEC-KO} HPM mice ($P < 0.01$). Compared with WT MESA mice, FADD levels were increased in A20^{IEC-KO} MESA mice ($P < 0.05$) (Figure 4F).

Co-expression of A20/TRADD and A20/RIP1 in intestinal epithelial tissues across groups

Co-expression of A20/TRADD: Cell nuclei stained blue. Regions rich in A20 expression stained green while those rich in TRADD stained red. Co-expression of A20 and TRADD stained yellow (red and green fluorescence). In WT NC mice, green fluorescence predominated (Figure 5A). In WT MC mice, red fluorescence predominated along with sparse yellow staining (Figure 5B). In WT MESA mice,

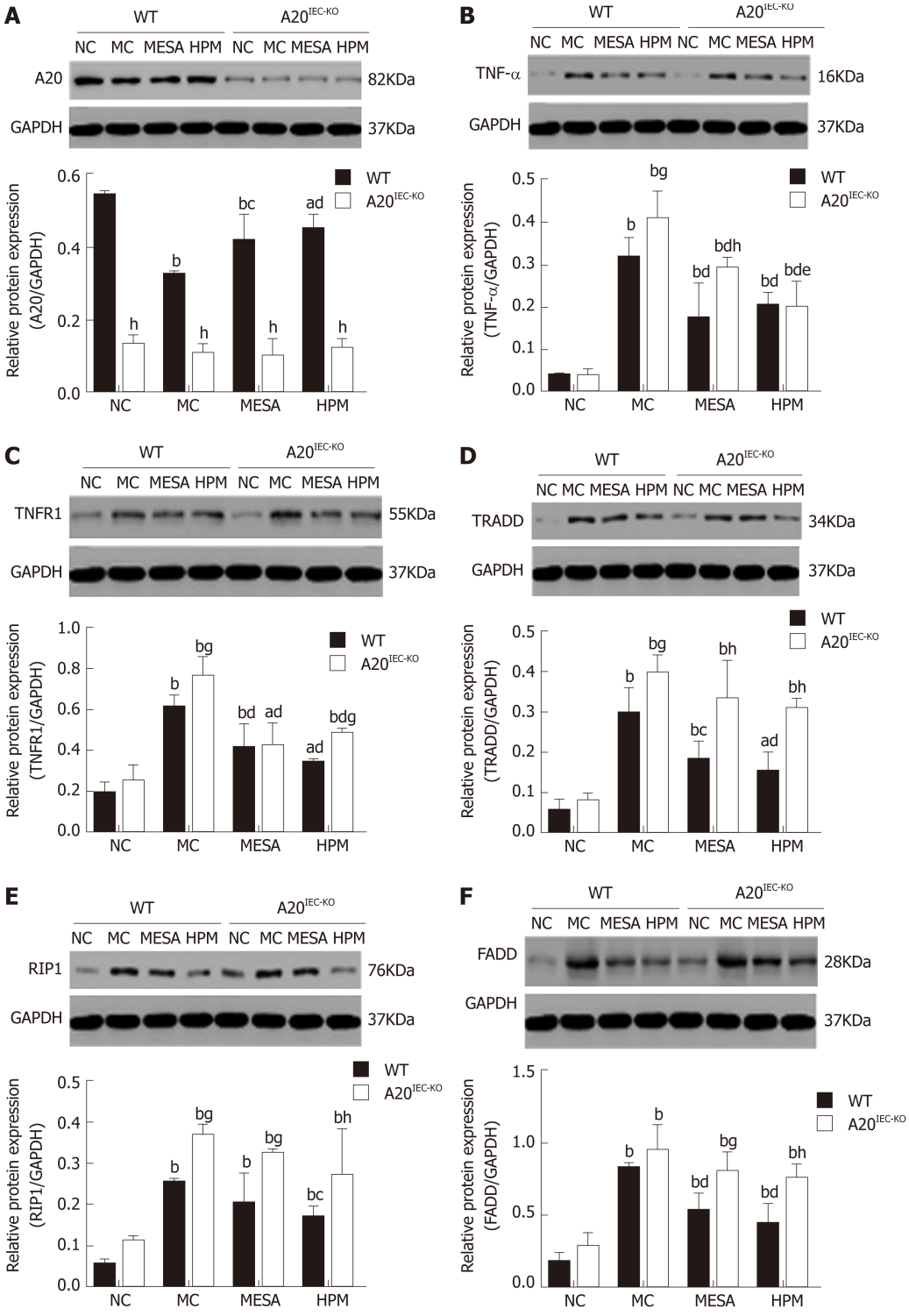

Figure 4 Expression levels of A20, tumor necrosis factor alpha, tumor necrosis factor receptor 1, tumor necrosis factor receptor 1-associated death domain, receptor-interacting protein 1, and FAS-associated death domain protein across groups. Data are presented as the mean ± standard deviation (n = 10). Data were evaluated for statistical significance using one-way analysis of variance and are represented as follows: $^{a}P < 0.05$, $^{b}P < 0.01$ as compared to normal contro; $^{c}P < 0.05$, $^{d}P < 0.01$ as compared to model control; $^{e}P < 0.05$, $^{f}P < 0.01$ as compared to mesalazine; $^{g}P < 0.05$, $^{h}P < 0.01$ as compared to wild type. TNFR1: Tumor necrosis factor receptor 1; RIP1: Receptor-interacting protein 1; TNF-α: Tumor necrosis factor alpha; TRADD: Tumor necrosis factor receptor 1-associated death domain; FADD: FAS-associated death domain; WT: Wild type; NC: Normal control; MC: Model control; MESA: Mesalazine; HPM: Herbs-partitioned moxibustion.

sparse yellow fluorescence predominated (Figure 5C). In WT HPM mice, immunofluorescence mainly revealed yellow fluorescence (Figure 5D). In A20^{IEC-KO} NC, MC, MESA, and HPM mice, red fluorescence predominated (Figure 5E-H).

In WT groups, compared with NC mice, A20 levels were significantly decreased in MC, MESA, and HPM mice ($P_{MC} < 0.01$, $P_{MESA} < 0.01$, $P_{HPM} < 0.01$). Compared with MC mice, expression of A20 was significantly increased in HPM mice ($P < 0.01$) and

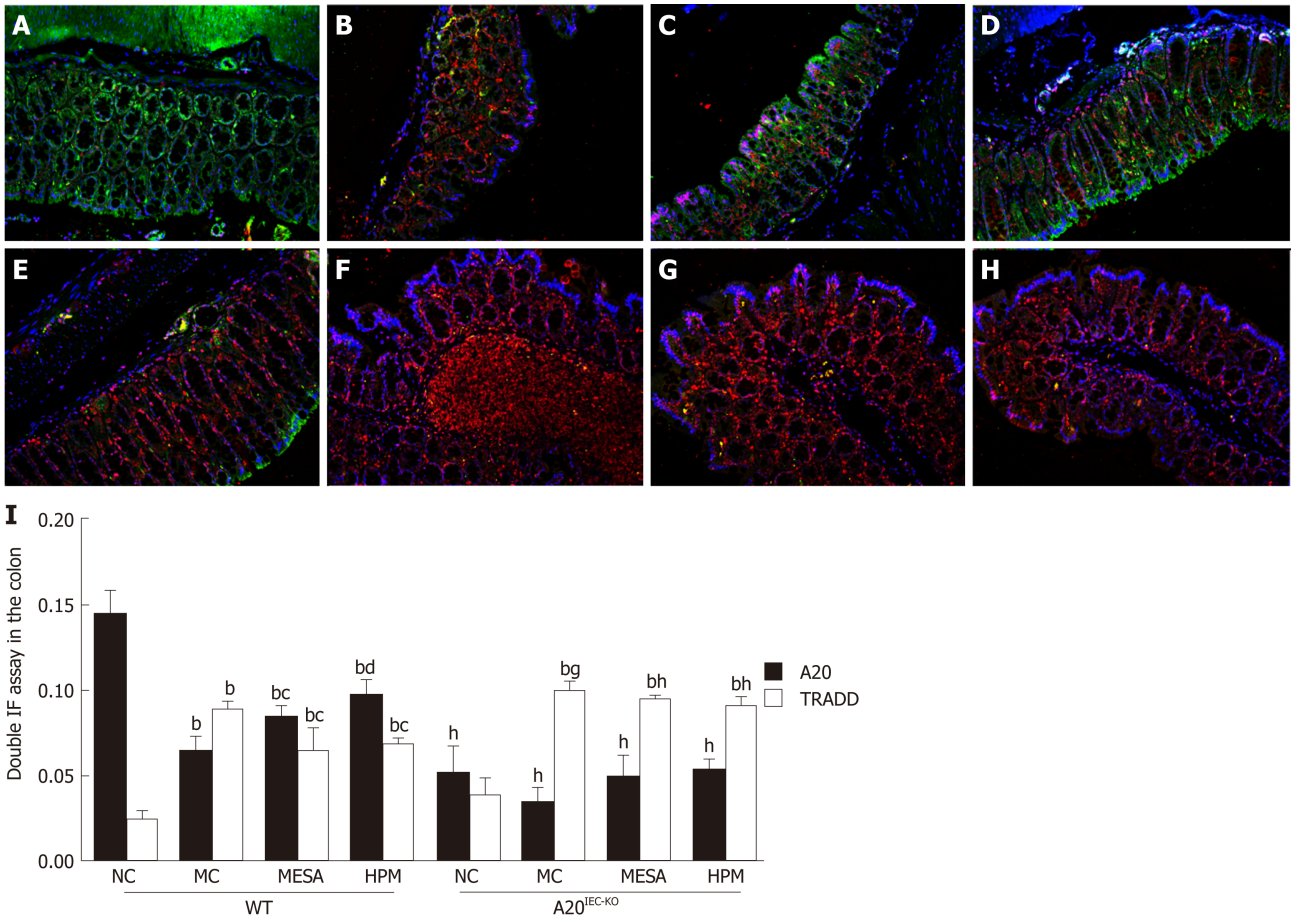

Figure 5 Co-expression of A20/tumor necrosis factor receptor 1-associated death domain in the intestinal epithelium of mice across groups. A: Wild-type mice in normal control group; B: Wild-type mice in model control group; C: Wild-type mice in mesalazine group; D: Wild-type mice in herbs-partitioned moxibustion group; E: A20^{IEC-KO} mice in normal control group; F: A20^{IEC-KO} mice in model control group; G: A20^{IEC-KO} mice in mesalazine group; H: A20^{IEC-KO} mice in herbs-partitioned moxibustion group. Data are presented as the mean ± standard deviation (n = 10). Data were evaluated for statistical significance using one-way analysis of variance and are represented as follows: $^{a}P < 0.05$, $^{b}P < 0.01$ as compared to normal contro; $^{c}P < 0.05$, $^{d}P < 0.01$ as compared to model control; $^{e}P < 0.05$, $^{f}P < 0.01$ as compared to mesalazine; $^{g}P < 0.05$, $^{h}P < 0.01$ as compared to wild type. TRADD: Tumor necrosis factor receptor 1-associated death domain; WT: Wild type; NC: Normal control; MC: Model control; MESA: Mesalazine; HPM: Herbs-partitioned moxibustion.

increased in those of the MESA group ($P < 0.05$). Compared with MESA mice, no difference in A20 levels in those of HPM mice was noted ($P > 0.05$) (Figure 5I). In A20^{IEC-KO} mice, no difference of A20 levels was noted among each group ($P > 0.05$) (Figure 5I). Compared with each corresponding group of WT mice, expression of A20 was significantly decreased in A20^{IEC-KO} mice ($P < 0.01$) (Figure 5I).

In WT groups, compared with NC mice, TRADD levels were significantly increased in MC, MESA, and HPM mice ($P_{MC} < 0.01$, $P_{MESA} < 0.01$, $P_{HMP} < 0.01$). Compared with MC mice, TRADD levels were decreased in mice of the MESA and HPM groups ($P_{MESA} < 0.05$, $P_{HPM} < 0.05$). Compared with MESA mice, no difference in TRADD levels was found in HPM mice ($P > 0.05$) (Figure 5I). In A20^{IEC-KO} groups, compared with NC mice, TRADD levels were significantly increased in MC, MESA, and HPM mice ($P_{MC} < 0.01$, $P_{MESA} < 0.01$, $P_{HPM} < 0.01$). No difference in TRADD levels were noted among MC, MESA, and HPM mice ($P > 0.05$) (Figure 5I). Compared with WT MC mice, TRADD levels were increased in A20^{IEC-KO} MC mice ($P < 0.05$). Compared with WT HPM and MESA mice, TRADD levels were significantly increased in mice of corresponding A20^{IEC-KO} groups ($P_{HPM} < 0.01$, $P_{MESA} < 0.01$) (Figure 5I).

Co-expression of A20/RIP1: Figure 6A-H shows that the nuclei exhibited blue fluorescence while regions rich in A20 and RIP1 stained green and red, respectively. Regions co-expressing A20 and RIP1 mainly stained yellow. In WT NC mice, imaged regions mainly stained green, occasionally intermixed with yellow fluorescence (Figure 6A). In WT MC mice, imaged regions stained mainly red and yellow (Figure 6B). In WT MESA mice, imaged regions mainly stained green (Figure 6C). In WT HPM mice, imaged regions mainly stained yellow (Figure 6D). In A20^{IEC-KO} NC mice, sparse red and green fluorescence was apparent (Figure 6E). In A20^{IEC-KO} MC, MESA, and HPM group mice, red fluorescence predominated (Figure 6F-H).

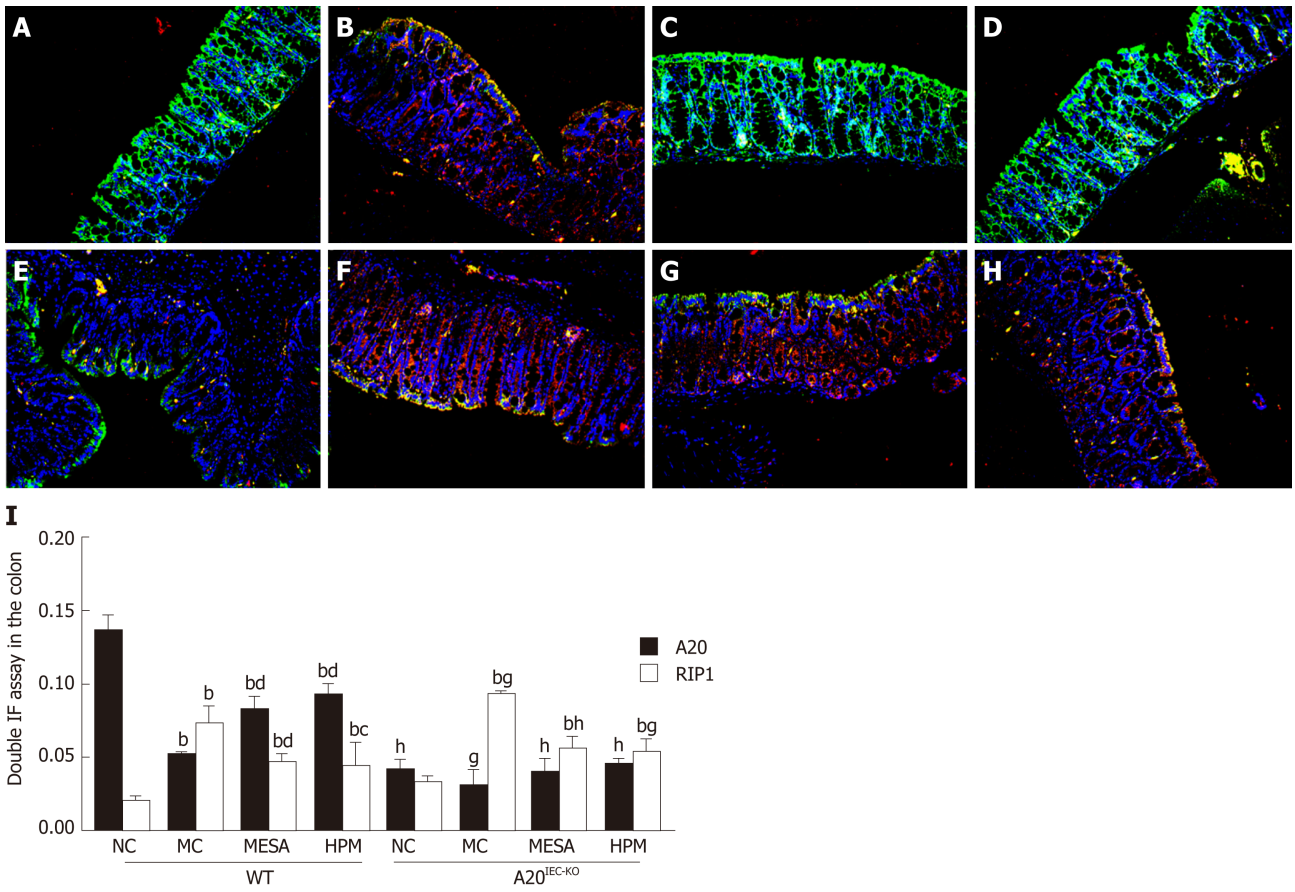

Figure 6 Co-expression of A20/receptor-interacting protein 1 in the intestinal epithelium of mice across groups. A: Wild-type mice in normal control group; B: Wild-type mice in model control group; C: Wild-type mice in mesalazine group; D: Wild-type mice in herbs-partitioned moxibustion group; E: A20^{IEC-KO} mice in normal control group; F: A20^{IEC-KO} mice in model control group; G: A20^{IEC-KO} mice in mesalazine group; H: A20^{IEC-KO} mice in herbs-partitioned moxibustion group. Data are presented as the mean ± standard deviation (n = 10). Data were evaluated for statistical significance using one-way analysis of variance and are represented as follows: $^{a}P < 0.05$, $^{b}P < 0.01$ as compared to normal control; $^{c}P < 0.05$, $^{d}P < 0.01$ as compared to model control; $^{e}P < 0.05$, $^{f}P < 0.01$ as compared to mesalazine; $^{g}P < 0.05$, $^{h}P < 0.01$ as compared to wild type. RIP1: Receptor-interacting protein 1; WT: Wild type; NC: Normal control; MC: Model control; MESA: Mesalazine; HPM: Herbs-partitioned moxibustion.

In WT groups, compared with NC mice, A20 expression was significantly decreased in MC, MESA, and HPM mice ($P_{MC} < 0.01$, $P_{MESA} < 0.01$, $P_{HPM} < 0.01$). A20 levels were significantly increased in HPM and MESA mice ($P_{HPM} < 0.01$, $P_{MESA} < 0.01$) as compared to MC mice. Compared with MESA mice, no difference in levels of A20 were found in HPM mice ($P > 0.05$). In A20^{IEC-KO} groups, no differences in A20 levels were found among groups ($P > 0.05$). Compared with each corresponding group of WT mice, A20 levels were significantly decreased in A20^{IEC-KO} NC, MESA, and HPM mice ($P_{NC} < 0.01$, $P_{MESA} < 0.01$, $P_{HPM} < 0.01$) and decreased in MC mice ($P_{MC} < 0.05$) (Figure 6I).

In WT groups, compared with NC mice, RIP1 levels were significantly increased in MC, MESA, and HPM mice ($P_{MC} < 0.01$, $P_{MESA} < 0.01$, $P_{HMP} < 0.01$). Compared with MC mice, RIP1 levels were significantly decreased in MESA mice ($P < 0.01$) and decreased in HPM mice ($P < 0.05$). Compared with MESA mice, no difference in RIP1 levels were noted in HPM mice ($P > 0.05$) (Figure 6I). In A20^{IEC-KO} groups, compared with NC mice, RIP1 levels were significantly increased in MC, MESA, and HPM mice ($P_{MC} < 0.01$, $P_{MESA} < 0.01$, $P_{HPM} < 0.01$). No difference in RIP1 levels was found among MC, MESA, and HPM mice ($P > 0.05$) (Figure 6I). Compared with WT NC mice, no difference in RIP1 levels was found in A20^{IEC-KO} NC mice ($P > 0.05$). Compared with WT MC mice, RIP1 expression was increased in A20^{IEC-KO} MC mice ($P < 0.05$). Compared with WT MESA mice, RIP1 expression was significantly increased in mice of the corresponding A20^{IEC-KO} group ($P_{MESA} < 0.01$). Compared with WT HPM mice, RIP1 levels were increased in A20^{IEC-KO} HPM mice ($P_{HPM} < 0.05$) (Figure 6I).

DISCUSSION

Although the etiology of Crohn's disease is still unknown, excessive apoptosis of intestinal epithelial cells leads to villus atrophy and epithelial destruction, which plays a central role in the pathogenesis of the disease[32,33]. A20, as an intestinal epithelium protector, is widely known for its functions in maintaining the epithelial barrier stability in inflammatory conditions. In Crohn's disease patients, there is an excessive inflammatory response and insufficient upregulation of A20 expression[34]. Our previous studies have indicated that HPM plays a beneficial role in Crohn's disease by decreasing intestinal epithelium apoptosis[29]. However, whether the effect of HPM is through A20 has not been determined. In the present study, we examined the anti-apoptotic properties of A20, confirmed its protective role in the intestinal epithelial barrier, and explored whether the effect of HPM in reducing intestinal epithelium apoptosis is through upregulating A20 levels in apoptotic signaling in a TNBS-induced Crohn's disease mouse model in WT and A20^{IEC-KO} lineages.

Aberrant apoptosis of intestinal epithelial cells lacking the A20 gene leads to increased intestinal epithelial permeability in Crohn's disease patients[35-37]. In the present study, we found that the intestinal epithelial cell apoptosis percentage was significantly increased in the Crohn's disease model of A20^{IEC-KO} mice ($P < 0.01$); moreover, serum endotoxin level was upregulated in this lineage ($P < 0.05$). Accordingly, H&E staining analysis showed that the intestinal epithelial barrier was severely damaged in the Crohn's disease model of A20^{IEC-KO} mice, consistent with the Lars Vereecke's report[13]. A previous study showed that HPM reduces intestinal epithelial apoptosis in a Crohn's disease mouse model[29]. The present study indicated that after treatment with HPM, despite improved intestinal morphological changes with decreased intestinal epithelial cell apoptosis percentages and endotoxin levels in A20^{IEC-KO} mice, a more significant improvement was detected in WT mice compared with A20^{IEC-KO} mice ($P < 0.01$). These findings suggested that upregulated A20 can protect intestinal epithelial barrier function and initially confirmed that HPM can upregulate A20 expression to protect the intestinal epithelial barrier in Crohn's disease.

The anti-apoptotic function of A20 has been found to inhibit the sequential signaling complexes of the TNF-α/TNFR1 apoptotic pathway upstream of caspase 8[38]. When TNFR1 binds to TNF-α, the death domain of TNFR1 enables the recruitment of TRADD and RIP1 proteins and their assembly with FADD to activate caspase-8 and induce apoptosis[39-41]. Therefore, we measured the protein expression levels of TNF-α, TNFR1, TRADD, RIP1, and FADD in the apoptotic pathway. The present study found no differences in TNF-α, TNFR1, TRADD, RIP1, or FADD levels among A20^{IEC-KO} NC mice, revealing that A20^{IEC-KO} NC intestinal epithelial cells do not spontaneously undergo apoptosis, in agreement with prior research by Lars Vereecke *et al*[13]. We previously reported that HPM and mild moxibustion downregulate TNF-α and TNFR1 expression levels and decrease intestinal epithelial cell apoptosis in Crohn's disease[29]. Here, we found that when A20 was upregulated in WT mice, TNF-α expression was decreased after HPM treatment in both WT and A20^{IEC-KO} Crohn's disease mice. Interestingly, TNF-α expression levels were not different in A20^{IEC-KO} and WT HPM mice. These results may indicate that HPM could downregulate TNF-α, which is consistent with our previous study[29], but the mechanism enacted by HPM in regulating TNF-α is not specifically associated with A20. TNFR1, TRADD, and RIP1 levels in A20^{IEC-KO} MC mice were found to be increased compared with those in WT mice, suggesting that A20^{IEC-KO} mice are hypersensitive to TNF-α-induced intestinal epithelial apoptosis, consistent with Vereecke's research[14]. Western blot analysis revealed that HPM significantly decreased the expression levels of TNFR1, TRADD, RIP1, and FADD in WT mice but had no effect on the levels of those proteins in A20^{IEC-KO} mice. All of these results indicated that although HPM can downregulate the expression levels of TNFR1, TRADD, RIP1, and FADD, the upregulated expression of A20 by HPM can downregulate TNFR1, TRADD, and RIP1 signaling molecules in the apoptotic pathway.

As TRADD and RIP1 play critical roles in the TNFR1-related signaling apoptotic pathway, we further observed the role of A20 in affecting TRADD and RIP1 expression[12]. A study showed that ligand-dependent association of RIP1 with TNFR1 was significantly reduced in A20-expressing cells in TNF-α-induced apoptosis. Furthermore, the recruitment of TRADD to the TNFR1 complex was also inhibited by A20[42]. In the present study, immunofluorescence showed a predominantly green color with a few yellow areas in intestinal epithelial tissue of the WT HPM group. The imaging data revealed co-expression of A20/TRADD and A20/RIP1 in WT HPM mice and decreased expression of TRADD and RIP1 along with increased expression of A20 in WT HPM mice. In A20^{IEC-KO} HPM mice, immunofluorescence showed a predominantly red color in intestinal epithelial tissue, suggesting a significant amount of TRADD and RIP1 expression without A20 expression. These results may identify a close association of A20, TRADD, and RIP1 within the TNF-α/TNFR1 apoptotic

pathway in a Crohn's disease mouse model. Our findings indicated that HPM upregulates the A20 level, which may affect the expression levels of TRADD and RIP1 in the apoptotic pathway.

In conclusion, HPM in treating Crohn's disease functions possibly via upregulation of the A20 expression level, resulting in downregulation of TNFR1, TRADD, and RIP1 to alleviate increased cell apoptosis in the intestinal epithelial barrier in Crohn's disease.

ARTICLE HIGHLIGHTS

Research background

A20, as an intestinal epithelium protector, plays a critical role in anti-apoptosis in Crohn's disease. Previous studies have indicated a beneficial role of herbs-partitioned moxibustion (HPM) in Crohn's disease by decreasing intestinal epithelial apoptosis. However, whether the effect of HPM is through A20 is unclear.

Research motivation

Our findings will suggest a role of HPM in regulating A20 level in anti-apoptotic pathway in the intestinal epithelium of mice with Crohn's disease.

Research objectives

To explore whether HPM alleviates cell apoptosis in the intestinal epithelium by upregulating A20 level in Crohn's disease.

Research methods

Two types of mice were included in this study, namely, mice with A20 deletion in intestinal epithelial cells ($A20^{IEC\text{-}KO}$) and wild-type mice. Both of them were randomly divided into normal control (NC), model control (MC), mesalazine (MESA), and HPM groups. 2,4,6-trinitrobenzene sulfonic acid (TNBS) was administered to establish a Crohn's disease model in the two types. The morphology of the colonic mucosa, serum endotoxin, apoptosis of epithelial cells, protein levels of A20 and tumor necrosis factor receptor (TNFR) 1-related signaling molecules, co-expression of A20 and TNFR1-associated death domain (TRADD), and co-expression of A20 and receptor-interacting protein (RIP) 1 were observed. All data are presented as the mean ± standard deviation.

Research results

Compared with $A20^{IEC\text{-}KO}$ mice, wild-type mice in the HPM group showed that damage of intestinal epithelial barrier was improved, serum endotoxin levels were significantly downregulated ($P < 0.01$), apoptosis percentages were significantly decreased ($P < 0.01$), A20 level was significantly upregulated ($P < 0.01$), and TNFR1, TRADDD, and RIP1 levels were downregulated ($P_{TNF\text{-}a} < 0.01$, $P_{TNFR1} < 0.05$, $P_{TRADD} < 0.05$, $P_{RIP1} < 0.05$). In addition, the co-expression of A20/TRADD and A20/RIP1 showed a predominant yellow fluorescence in WT HPM mice, while a predominantly red fluorescence was noted in $A20^{IEC\text{-}KO}$ HPM mice.

Research conclusions

HPM can upregulate A20 level, resulting in decreased expression of TNFR1, TRADD, and RIP1 to alleviate aberrant cell apoptosis in the intestinal epithelial barrier in Crohn's disease.

Research perspectives

Effect of HPM in decreasing cell apoptosis of intestinal epithelial cells is through upregulating A20 level in Crohn's disease.

REFERENCES

1 **Matsuoka K**, Kobayashi T, Ueno F, Matsui T, Hirai F, Inoue N, Kato J, Kobayashi K, Kobayashi K, Koganei K, Kunisaki R, Motoya S, Nagahori M, Nakase H, Omata F, Saruta M, Watanabe T, Tanaka T, Kanai T, Noguchi Y, Takahashi KI, Watanabe K, Hibi T, Suzuki Y, Watanabe M, Sugano K, Shimosegawa T. Evidence-based clinical practice guidelines for inflammatory bowel disease. *J Gastroenterol* 2018; **53**: 305-353 [PMID: 29429045 DOI: 10.1007/s00535-018-1439-1]

2 **Kaplan GG**. The global burden of IBD: from 2015 to 2025. *Nat Rev Gastroenterol Hepatol* 2015; **12**: 720-727 [PMID: 26323879 DOI: 10.1038/nrgastro.2015.150]

3 **Ng SC**, Shi HY, Hamidi N, Underwood FE, Tang W, Benchimol EI, Panaccione R, Ghosh S, Wu JCY, Chan FKL, Sung JJY, Kaplan GG. Worldwide incidence and prevalence of inflammatory bowel disease in the 21st century: a systematic review of population-based studies. *Lancet* 2018; **390**: 2769-2778 [PMID: 29050646 DOI: 10.1016/S0140-6736(17)32448-0]

4 **Ng SC**, Kaplan GG, Tang W, Banerjee R, Adigopula B, Underwood FE, Tanyingoh D, Wei SC, Lin WC, Lin HH, Li J, Bell S, Niewiadomski O, Kamm MA, Zeng Z, Chen M, Hu P, Ong D, Ooi CJ, Ling KL, Miao Y, Miao J, Janaka de Silva H, Niriella M, Aniwan S, Limsrivilai J, Pisespongsa P, Wu K, Yang H, Ng KK, Yu HH, Wang Y, Ouyang Q, Abdullah M, Simadibrata M, Gunawan J, Hilmi I, Lee Goh K, Cao Q, Sheng H, Ong-Go A, Chong VH, Ching JYL, Wu JCY, Chan FKL, Sung JJY. Population Density and Risk of Inflammatory Bowel Disease: A Prospective Population-Based Study in 13 Countries or Regions in Asia-Pacific. *Am J Gastroenterol* 2019; **114**: 107-115 [PMID: 30177785 DOI:

10.1038/s41395-018-0233-2]
5 **Ananthakrishnan AN**. Epidemiology and risk factors for IBD. *Nat Rev Gastroenterol Hepatol* 2015; **12**: 205-217 [PMID: 25732745 DOI: 10.1038/nrgastro.2015.34]
6 **Kaser A**, Zeissig S, Blumberg RS. Inflammatory bowel disease. *Annu Rev Immunol* 2010; **28**: 573-621 [PMID: 20192811 DOI: 10.1146/annurev-immunol-030409-101225]
7 **Clevers H**. The intestinal crypt, a prototype stem cell compartment. *Cell* 2013; **154**: 274-284 [PMID: 23870119 DOI: 10.1016/j.cell.2013.07.004]
8 **Bullen TF**, Forrest S, Campbell F, Dodson AR, Hershman MJ, Pritchard DM, Turner JR, Montrose MH, Watson AJ. Characterization of epithelial cell shedding from human small intestine. *Lab Invest* 2006; **86**: 1052-1063 [PMID: 16909128 DOI: 10.1038/labinvest.3700464]
9 **Grabinger T**, Luks L, Kostadinova F, Zimberlin C, Medema JP, Leist M, Brunner T. Ex vivo culture of intestinal crypt organoids as a model system for assessing cell death induction in intestinal epithelial cells and enteropathy. *Cell Death Dis* 2014; **5**: e1228 [PMID: 24832600 DOI: 10.1038/cddis.2014.183]
10 **Suzuki T**. Regulation of intestinal epithelial permeability by tight junctions. *Cell Mol Life Sci* 2013; **70**: 631-659 [PMID: 22782113 DOI: 10.1007/s00018-012-1070-x]
11 **Zeissig S**, Bojarski C, Buergel N, Mankertz J, Zeitz M, Fromm M, Schulzke JD. Downregulation of epithelial apoptosis and barrier repair in active Crohn's disease by tumour necrosis factor alpha antibody treatment. *Gut* 2004; **53**: 1295-1302 [PMID: 15306588 DOI: 10.1136/gut.2003.036632]
12 **Park YH**, Jeong MS, Jang SB. Death domain complex of the TNFR-1, TRADD, and RIP1 proteins for death-inducing signaling. *Biochem Biophys Res Commun* 2014; **443**: 1155-1161 [PMID: 24361886 DOI: 10.1016/j.bbrc.2013.12.068]
13 **Vereecke L**, Vieira-Silva S, Billiet T, van Es JH, Mc Guire C, Slowicka K, Sze M, van den Born M, De Hertogh G, Clevers H, Raes J, Rutgeerts P, Vermeire S, Beyaert R, van Loo G. A20 controls intestinal homeostasis through cell-specific activities. *Nat Commun* 2014; **5**: 5103 [PMID: 25267258 DOI: 10.1038/ncomms6103]
14 **Vereecke L**, Sze M, Mc Guire C, Rogiers B, Chu Y, Schmidt-Supprian M, Pasparakis M, Beyaert R, van Loo G. Enterocyte-specific A20 deficiency sensitizes to tumor necrosis factor-induced toxicity and experimental colitis. *J Exp Med* 2010; **207**: 1513-1523 [PMID: 20530205 DOI: 10.1084/jem.20092474]
15 **Coornaert B**, Carpentier I, Beyaert R. A20: central gatekeeper in inflammation and immunity. *J Biol Chem* 2009; **284**: 8217-8221 [PMID: 19008218 DOI: 10.1074/jbc.R800032200]
16 **Zhang M**, Peng LL, Wang Y, Wang JS, Liu J, Liu MM, Hu J, Song B, Yang HB. Roles of A20 in autoimmune diseases. *Immunol Res* 2016; **64**: 337-344 [PMID: 26135958 DOI: 10.1007/s12026-015-8677-6]
17 **Wertz IE**, Newton K, Seshasayee D, Kusam S, Lam C, Zhang J, Popovych N, Helgason E, Schoeffler A, Jeet S, Ramamoorthi N, Kategaya L, Newman RJ, Horikawa K, Dugger D, Sandoval W, Mukund S, Zindal A, Martin F, Quan C, Tom J, Fairbrother WJ, Townsend M, Warming S, DeVoss J, Liu J, Dueber E, Caplazi P, Lee WP, Goodnow CC, Balazs M, Yu K, Kolumam G, Dixit VM. Phosphorylation and linear ubiquitin direct A20 inhibition of inflammation. *Nature* 2015; **528**: 370-375 [PMID: 26649818 DOI: 10.1038/nature16165]
18 **Hammer GE**, Turer EE, Taylor KE, Fang CJ, Advincula R, Oshima S, Barrera J, Huang EJ, Hou B, Malynn BA, Reizis B, DeFranco A, Criswell LA, Nakamura MC, Ma A. Expression of A20 by dendritic cells preserves immune homeostasis and prevents colitis and spondyloarthritis. *Nat Immunol* 2011; **12**: 1184-1193 [PMID: 22019834 DOI: 10.1038/ni.2135]
19 **Bellail AC**, Olson JJ, Yang X, Chen ZJ, Hao C. A20 ubiquitin ligase-mediated polyubiquitination of RIP1 inhibits caspase-8 cleavage and TRAIL-induced apoptosis in glioblastoma. *Cancer Discov* 2012; **2**: 140-155 [PMID: 22585859 DOI: 10.1158/2159-8290.CD-11-0172]
20 **Cheifetz AS**. Management of active Crohn disease. *JAMA* 2013; **309**: 2150-2158 [PMID: 23695484 DOI: 10.1001/jama.2013.4466]
21 **Rahier JF**, Magro F, Abreu C, Armuzzi A, Ben-Horin S, Chowers Y, Cottone M, de Ridder L, Doherty G, Ehehalt R, Esteve M, Katsanos K, Lees CW, Macmahon E, Moreels T, Reinisch W, Tilg H, Tremblay L, Veereman-Wauters G, Viget N, Yazdanpanah Y, Eliakim R, Colombel JF; European Crohn's and Colitis Organisation (ECCO). Second European evidence-based consensus on the prevention, diagnosis and management of opportunistic infections in inflammatory bowel disease. *J Crohns Colitis* 2014; **8**: 443-468 [PMID: 24613021 DOI: 10.1016/j.crohns.2013.12.013]
22 **Kim YS**, Jung SA, Lee KM, Park SJ, Kim TO, Choi CH, Kim HG, Moon W, Moon CM, Song HK, Na SY, Yang SK; Korean Association for the Study of Intestinal Diseases (KASID). Impact of inflammatory bowel disease on daily life: an online survey by the Korean Association for the Study of Intestinal Diseases. *Intest Res* 2017; **15**: 338-344 [PMID: 28670230 DOI: 10.5217/ir.2017.15.3.338]
23 **Gearry RB**, Barclay ML, Burt MJ, Collett JA, Chapman BA. Thiopurine drug adverse effects in a population of New Zealand patients with inflammatory bowel disease. *Pharmacoepidemiol Drug Saf* 2004; **13**: 563-567 [PMID: 15317038 DOI: 10.1002/pds.926]
24 **Moja L**, Danese S, Fiorino G, Del Giovane C, Bonovas S. Systematic review with network meta-analysis: comparative efficacy and safety of budesonide and mesalazine (mesalamine) for Crohn's disease. *Aliment Pharmacol Ther* 2015; **41**: 1055-1065 [PMID: 25864873 DOI: 10.1111/apt.13190]
25 **Hanauer SB**, Korelitz BI, Rutgeerts P, Peppercorn MA, Thisted RA, Cohen RD, Present DH. Postoperative maintenance of Crohn's disease remission with 6-mercaptopurine, mesalamine, or placebo: a 2-year trial. *Gastroenterology* 2004; **127**: 723-729 [PMID: 15362027 DOI: 10.1053/j.gastro.2004.06.002]
26 **Shang HX**, Wang AQ, Bao CH, Wu HG, Chen WF, Wu LY, Ji R, Zhao JM, Shi Y. Moxibustion combined with acupuncture increases tight junction protein expression in Crohn's disease patients. *World J Gastroenterol* 2015; **21**: 4986-4996 [PMID: 25945013 DOI: 10.3748/wjg.v21.i16.4986]
27 **Bao C**, Liu P, Liu H, Jin X, Calhoun VD, Wu L, Shi Y, Zhang J, Zeng X, Ma L, Qin W, Zhang J, Liu X, Tian J, Wu H. Different brain responses to electro-acupuncture and moxibustion treatment in patients with Crohn's disease. *Sci Rep* 2016; **6**: 36636 [PMID: 27857211 DOI: 10.1038/srep36636]
28 **Bao CH**, Zhao JM, Liu HR, Lu Y, Zhu YF, Shi Y, Weng ZJ, Feng H, Guan X, Li J, Chen WF, Wu LY, Jin XM, Dou CZ, Wu HG. Randomized controlled trial: moxibustion and acupuncture for the treatment of Crohn's disease. *World J Gastroenterol* 2014; **20**: 11000-11011 [PMID: 25152604 DOI: 10.3748/wjg.v20.i31.11000]
29 **Bao CH**, Wu LY, Wu HG, Shi Y, Liu HR, Zhang R, Yu LQ, Wang JH. Moxibustion inhibits apoptosis and tumor necrosis factor-alpha/tumor necrosis factor receptor 1 in the colonic epithelium of Crohn's disease model rats. *Dig Dis Sci* 2012; **57**: 2286-2295 [PMID: 22531889 DOI: 10.1007/s10620-012-2161-0]

30 **Monteleone I**, Federici M, Sarra M, Franzè E, Casagrande V, Zorzi F, Cavalera M, Rizzo A, Lauro R, Pallone F, MacDonald TT, Monteleone G. Tissue inhibitor of metalloproteinase-3 regulates inflammation in human and mouse intestine. *Gastroenterology* 2012; **143**: 1277-1287.e4 [PMID: 22819866 DOI: 10.1053/j.gastro.2012.07.016]

31 **Xu SY**, Chen X. *Pharmacological Experiment Methodology*. Beijing: People's Health Publishing House 2002; 1184

32 **Günther C**, Neumann H, Neurath MF, Becker C. Apoptosis, necrosis and necroptosis: cell death regulation in the intestinal epithelium. *Gut* 2013; **62**: 1062-1071 [PMID: 22689519 DOI: 10.1136/gutjnl-2011-301364]

33 **Ruemmele FM**, Seidman EG, Lentze MJ. Regulation of intestinal epithelial cell apoptosis and the pathogenesis of inflammatory bowel disorders. *J Pediatr Gastroenterol Nutr* 2002; **34**: 254-260 [PMID: 11964947 DOI: 10.1097/00005176-200203000-00005]

34 **Zheng CF**, Huang Y. [Expression of zinc finger protein A20 in pediatric inflammatory bowel disease]. *Zhonghua Er Ke Za Zhi* 2011; **49**: 261-265 [PMID: 21624200]

35 **Di Sabatino A**, Ciccocioppo R, Luinetti O, Ricevuti L, Morera R, Cifone MG, Solcia E, Corazza GR. Increased enterocyte apoptosis in inflamed areas of Crohn's disease. *Dis Colon Rectum* 2003; **46**: 1498-1507 [PMID: 14605569 DOI: 10.1097/01.DCR.0000089118.20964.12]

36 **Schulzke JD**, Bojarski C, Zeissig S, Heller F, Gitter AH, Fromm M. Disrupted barrier function through epithelial cell apoptosis. *Ann N Y Acad Sci* 2006; **1072**: 288-299 [PMID: 17057208 DOI: 10.1196/annals.1326.027]

37 **Eder P**, Lykowska-Szuber L, Krela-Kazmierczak I, Stawczyk-Eder K, Zabel M, Linke K. The influence of infliximab and adalimumab on the expression of apoptosis-related proteins in lamina propria mononuclear cells and enterocytes in Crohn's disease - an immunohistochemical study. *J Crohns Colitis* 2013; **7**: 706-716 [PMID: 23021876 DOI: 10.1016/j.crohns.2012.09.006]

38 **Pearson JS**, Giogha C, Ong SY, Kennedy CL, Kelly M, Robinson KS, Lung TW, Mansell A, Riedmaier P, Oates CV, Zaid A, Mühlen S, Crepin VF, Marches O, Ang CS, Williamson NA, O'Reilly LA, Bankovacki A, Nachbur U, Infusini G, Webb AI, Silke J, Strasser A, Frankel G, Hartland EL. A type III effector antagonizes death receptor signalling during bacterial gut infection. *Nature* 2013; **501**: 247-251 [PMID: 24025841 DOI: 10.1038/nature12524]

39 **Hsu H**, Xiong J, Goeddel DV. The TNF receptor 1-associated protein TRADD signals cell death and NF-kappa B activation. *Cell* 1995; **81**: 495-504 [PMID: 7758105 DOI: 10.1016/0092-8674(95)90070-5]

40 **Hsu H**, Huang J, Shu HB, Baichwal V, Goeddel DV. TNF-dependent recruitment of the protein kinase RIP to the TNF receptor-1 signaling complex. *Immunity* 1996; **4**: 387-396 [PMID: 8612133 DOI: 10.1016/S1074-7613(00)80252-6]

41 **Ting AT**, Pimentel-Muiños FX, Seed B. RIP mediates tumor necrosis factor receptor 1 activation of NF-kappaB but not Fas/APO-1-initiated apoptosis. *EMBO J* 1996; **15**: 6189-6196 [PMID: 8947041 DOI: 10.1002/j.1460-2075.1996.tb01007.x]

42 **He KL**, Ting AT. A20 inhibits tumor necrosis factor (TNF) alpha-induced apoptosis by disrupting recruitment of TRADD and RIP to the TNF receptor 1 complex in Jurkat T cells. *Mol Cell Biol* 2002; **22**: 6034-6045 [PMID: 12167698 DOI: 10.1128/mcb.22.17.6034-6045.2002]

Published By Baishideng Publishing Group Inc
7041 Koll Center Parkway, Suite 160, Pleasanton, CA 94566, USA
Telephone: +1-925-2238242
Fax: +1-925-2238243
E-mail: bpgoffice@wjgnet.com
Help Desk:http://www.f6publishing.com/helpdesk
http://www.wjgnet.com